

Topological ac charge current and continuous invariant in the α - T_3 lattice under a periodically varying strain

Ruigang Li,¹ Jun-Feng Liu^{2,*} and Jun Wang^{3,†}

¹*School of Physics and Materials Science, Guangzhou University, Guangzhou 510006, China*

²*Department of Physics, School of Physics and Materials Science, Guangzhou University, Guangzhou 510006, China*

³*Department of Physics, Southeast University, Nanjing 210096, China*



(Received 5 January 2023; revised 7 August 2023; accepted 23 August 2023; published 5 September 2023)

Usually, robust invariants in physics take discrete values for the reason of topology, such as integers or fractions in the integer or fractional quantum Hall effect. Here, we show theoretically that the valley Chern number can be responsible for continuous invariants which are insensitive to most parameters, but continuously tunable by a critical parameter. We numerically calculate the ac charge current generated by a periodically varying strain in the α - T_3 lattice where the valley Chern number is continuously tunable by α . The periodically varying strain induces a valley-opposite ac pseudoelectric field which leads to a pure valley current in the longitudinal direction, and a charge current in the transverse direction via the topological valley Hall effect. The corresponding Hall pseudoconductance at the low-frequency limit equals the valley Chern number in gapped α - T_3 lattices and is robust against long-range disorders. This finding advances the understanding of the relation between invariants and topology, and also provides a scheme to test the quantum valley Hall effect.

DOI: [10.1103/PhysRevB.108.115403](https://doi.org/10.1103/PhysRevB.108.115403)

I. INTRODUCTION

It is well known that robust invariants in physics usually take discrete values, such as integers or fractions in the integer [1,2] or fractional quantum Hall effect [3,4], due to the topological origin. The natural question is whether there exists a continuous invariant which is insensitive to most parameters, but at the same time is continuously tunable by a critical parameter. It seems impossible for a well-defined topological number which should be an integer. But for a not-well-defined topological number, such as the valley Chern number [5,6], the number need not be an integer. For example, in the α - T_3 lattice which interpolates between the honeycomb lattice of graphene and the dice lattice [7–10], the valley Chern number can be continuous and tunable by the critical parameter α [11,12]. Most interestingly, the valley Chern number is still robust against fluctuations of model parameters except α . Therefore, it is desirable to explore the physical consequences of the robustness of the valley Chern number.

The valley Chern number is approximately well defined when the intervalley scattering is ignorable. But the detection of valley current is still quite challenging. The experimental observation of nonlocal conductance due to the quantum valley Hall effect in bilayer graphene is still controversial and far from quantization [13]. Fortunately, strain can act as a valley-opposite driving and generate a charge current instead of a valley current. In the α - T_3 lattice, strain can be described by an effective valley-opposite pseudovector potential as in graphene. The periodically varying strain will induce a

valley-opposite ac pseudoelectric field which leads to a charge current in the transverse direction via the quantum valley Hall effect [14]. The corresponding Hall pseudoconductance which relates the charge current to the pseudoelectric field is expected to equal the valley Chern number at the low-frequency limit in gapped α - T_3 lattices.

In this paper, we theoretically demonstrate the generation of a robust charge current in gapped α - T_3 lattices by a periodically varying strain as the result of the quantum valley Hall effect. The corresponding Hall pseudoconductance equals exactly the valley Chern number at the low-frequency limit which is continuously tunable by the critical parameter α . By applying uniaxial (shear) strain, we obtain a robust charge current response in the armchair (zigzag) direction in the frame of linear response theory. The Hall pseudoconductance is robust against the fluctuation of most parameters and long-range disorders.

II. MODEL AND LINEAR RESPONSE FORMALISM

In the α - T_3 lattice shown in Figs. 1(c) and 1(d), sites A and B form a honeycomb lattice, and sites C sit at the center of the hexagons and couple to sites B . The hopping energy between sites A and B is $t_{ab} = t_0 \cos \varphi$, and the hopping between sites B and C is $t_{bc} = t_0 \sin \varphi$. Here, $t_0 = 2.73$ eV is the same as that in graphene. The parameter α is defined as $\alpha = t_{bc}/t_{ab} = \tan \varphi$, and the hopping between sites A and C is ignored. This α - T_3 model interpolates between the honeycomb lattice of graphene ($\alpha = 0$) and the dice lattice ($\alpha = 1$) via the parameter α . The tight-binding Hamiltonian of the α - T_3 lattice can be written as

$$H = \sum_{(i,j),(j,k)} (t_{ab} a_i^\dagger b_j + t_{bc} b_j^\dagger c_k + \text{H.c.}), \quad (1)$$

*phjfliu@gzhu.edu.cn

†jwang@seu.edu.cn

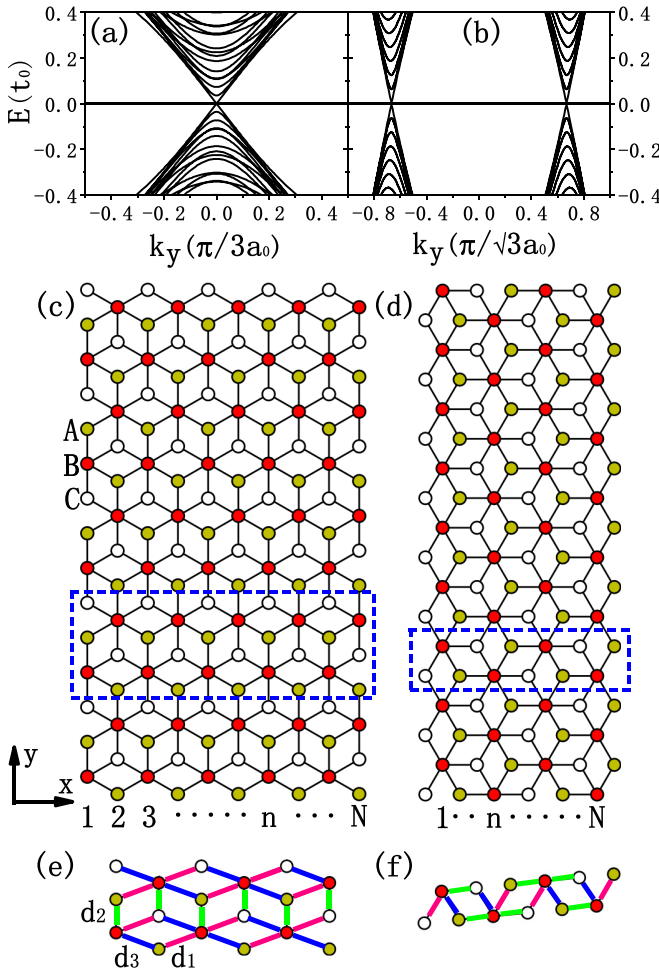


FIG. 1. The band structures of the (a) armchair and (b) zigzag α - T_3 ribbon ($N = 100$), with $k_x = 2\pi/(3\sqrt{3}a_0)$ and $k_x = 0$, respectively. The schematic of the (c) armchair and (d) zigzag α - T_3 ribbon. The supercells in the blue dotted rectangle contain N cells and the y direction is considered as the longitudinal direction. (e) The supercell ($N = 6$) of armchair α - T_3 ribbon after uniaxial deformation and (f) the supercell ($N = 4$) of zigzag α - T_3 ribbon after shear deformation. The bond lengths are changed from a_0 to d_χ , $\chi = 1$ (pink bonds), 2 (green bonds), 3 (blue bonds).

where a_i^\dagger (b_i^\dagger , c_i^\dagger) is the creation operator of the electron at site A (B , C).

For the convenience of checking the robustness against disorders, we consider armchair and zigzag α - T_3 ribbons with periodic boundary conditions to remove the edge effect. For an armchair ribbon with width N as shown in Fig. 1(c), the tight-binding Hamiltonian can be written as

$$H_A(\mathbf{k}) = \begin{bmatrix} I_1^A & O_1^A & 0 & \cdots & \cdots & \cdots & O_{1N}^A \\ O_1^{A\dagger} & I_2^A & O_2^A & \cdots & \cdots & \cdots & 0 \\ 0 & O_2^{A\dagger} & I_3^A & \cdots & \cdots & \cdots & 0 \\ \cdots & \cdots & \cdots & \cdots & \cdots & \cdots & \cdots \\ \cdots & \cdots & \cdots & O_{n-1}^{A\dagger} & I_n^A & O_n^A & \cdots \\ \cdots & \cdots & \cdots & \cdots & \cdots & \cdots & \cdots \\ O_{1N}^{A\dagger} & 0 & 0 & \cdots & \cdots & O_{N-1}^{A\dagger} & I_N^A \end{bmatrix}, \quad (2)$$

where

$$I_n^A = M + \begin{pmatrix} 0 & t_{ab}^y & 0 \\ t_{ab}^{y*} & 0 & t_{bc}^y \\ 0 & t_{bc}^{y*} & 0 \end{pmatrix}, \quad M = \begin{pmatrix} m_A & 0 & 0 \\ 0 & m_B & 0 \\ 0 & 0 & m_C \end{pmatrix},$$

$$O_n^A = \begin{pmatrix} 0 & t_{ab}^x & 0 \\ t_{ab}^{x*} & 0 & t_{bc}^x \\ 0 & t_{bc}^{x*} & 0 \end{pmatrix}, \quad O_{1N}^A = \begin{pmatrix} 0 & t_{ab}^{x0} & 0 \\ t_{ab}^{x0*} & 0 & t_{bc}^{x0} \\ 0 & t_{bc}^{x0*} & 0 \end{pmatrix}.$$

The supercell, shown in the blue dotted rectangle in Fig. 1(c), consists of N cells, and n is the cell index. The wave function of cell n can be written as $\psi_n = (a_n, b_n, c_n)^T$. I_n^A and O_n^A denote the intracell and intercell hopping matrices, respectively. $t_{ab(bc)}^y = t_{ab(bc)} e^{-ia_0 k_y}$ and $t_{ab(bc)}^x = t_{ab(bc)} e^{i\frac{a_0}{2} k_y}$ are hopping parameters of the armchair ribbon. $t_{ab(bc)}^{x0} = t_{ab(bc)} e^{i(\frac{a_0}{2} k_y + N \frac{\sqrt{3}a_0}{2} k_x)}$. M in I_n^A denotes the mass term, and m_A (m_B , m_C) is the extra on-site energy at site A (B , C). Without considering the mass term, the band structure of the armchair ribbon is shown in Fig. 1(a). Note that the band structure is independent of α .

When a time-dependent uniaxial strain is applied to the armchair ribbon along the zigzag direction, the instantaneous deformed bond lengths [see Fig. 1(e)] are respectively given as [15]

$$d_1 = d_3 = a_0[1 + (3 - \sigma)\epsilon(\tau)/4],$$

$$d_2 = a_0[1 - \sigma\epsilon(\tau)], \quad (3)$$

where $\epsilon(\tau) = \epsilon_0 \cos(\omega\tau)$ denotes a time-dependent uniaxial strain. ϵ_0 and ω are the amplitude and frequency of the strain, respectively. σ denotes the Poisson's ratio of the lattice, with the value $\sigma = 0.165$ [16]. The deformations will change the hopping parameters of the bonds. For a small deformation, the changes are much smaller than t_0 . The perturbation Hamiltonian can be written as

$$H_A'(\mathbf{k}, \tau) = \begin{bmatrix} I_1^{A'} & O_1^{A'} & 0 & \cdots & \cdots & \cdots & O_{1N}^{A'} \\ O_1^{A'\dagger} & I_2^{A'} & O_2^{A'} & \cdots & \cdots & \cdots & 0 \\ 0 & O_2^{A'\dagger} & I_3^{A'} & \cdots & \cdots & \cdots & 0 \\ \cdots & \cdots & \cdots & \cdots & \cdots & \cdots & \cdots \\ \cdots & \cdots & \cdots & O_{n-1}^{A'\dagger} & I_n^{A'} & O_n^{A'} & \cdots \\ \cdots & \cdots & \cdots & \cdots & \cdots & \cdots & \cdots \\ O_{N1}^{A'\dagger} & 0 & 0 & \cdots & \cdots & O_{N-1}^{A'\dagger} & I_N^{A'} \end{bmatrix}, \quad (4)$$

where

$$I_n^{A'} = \begin{pmatrix} 0 & t_{ab}^{y'} & 0 \\ t_{ab}^{y'/*} & 0 & t_{bc}^{y'} \\ 0 & t_{bc}^{y'/*} & 0 \end{pmatrix},$$

$$O_n^{A'} = \begin{pmatrix} 0 & t_{ab}^{x'} & 0 \\ t_{ab}^{x'/*} & 0 & t_{bc}^{x'} \\ 0 & t_{bc}^{x'/*} & 0 \end{pmatrix}, \quad O_{1N}^{A'} = \begin{pmatrix} 0 & t_{ab}^{x0'} & 0 \\ t_{ab}^{x0'/*} & 0 & t_{bc}^{x0'} \\ 0 & t_{bc}^{x0'/*} & 0 \end{pmatrix}.$$

Under the first-order approximation, the hopping parameters

are respectively written as

$$\begin{aligned} t_{ab(bc)}^{x'} &= -\beta(3 - \sigma)\epsilon(\tau)t_{ab(bc)}^x/4, \\ t_{ab(bc)}^{xo'} &= -\beta(3 - \sigma)\epsilon(\tau)t_{ab(bc)}^{xo}/4, \\ t_{ab(bc)}^{y'} &= \beta\sigma\epsilon(\tau)t_{ab(bc)}^y. \end{aligned} \quad (5)$$

In this study, the Grüneisen parameter is set to be $\beta = 3.37$ [15–17]. For space limitation, the Hamiltonian of the zigzag α - T_3 ribbon is shown in Appendix A. Without the mass term, the band structure of the zigzag ribbon is shown in Fig. 1(b). According to linear response theory, the ac charge current response along the longitudinal direction (y direction) can be calculated by

$$J_y(\tau) = -\sum_{kjj'} \frac{J_{jj'}^y(\mathbf{k})H'_{jj'}(\mathbf{k}, \tau)(f_{kj} - f_{kj'})}{\hbar\omega + E_{kj} - E_{kj'} + i\eta}, \quad (6)$$

where $E_{k(j')}$ is the $j(j')$ th eigenenergy of the unperturbed Hamiltonian, for a fixed \mathbf{k} . Assuming ϕ_{kj} is the corresponding eigenwave function, $J_{jj'}^y(\mathbf{k})$ and $H'_{jj'}(\mathbf{k}, \tau)$ in Eq. (6) are detailedly written as $J_{jj'}^y(\mathbf{k}) = \frac{e}{\hbar}\phi_{kj}^\dagger \frac{\partial H(\mathbf{k})}{\partial k_y} \phi_{kj'}$ and $H'_{jj'}(\mathbf{k}, \tau) = \phi_{kj'}^\dagger H'_{A/Z}(\mathbf{k}, \tau)\phi_{kj}$, respectively. η is a positive infinitesimal. The Fermi distribution can be written as $f_{kj} = [1 + e^{-(E_{kj} - \mu)/k_B T}]^{-1}$, where μ and T represent the Fermi energy and temperature, respectively. The deduction of Eq. (6) is shown in Appendix C.

Similar to graphene, when the uniaxial (shear) strain is applied to the armchair (zigzag) α - T_3 ribbon along the zigzag direction, a pseudovector potential \mathbf{A} will be effectively introduced and coupled with opposite signs to two valleys due to the time-reversal symmetry. When a time-dependent strain is applied, the corresponding pseudoelectric field would be [14,18,19]

$$\mathbf{E}(\tau) = -\frac{\partial \mathbf{A}(\tau)}{\partial \tau} = -i\omega \frac{\hbar}{e} \delta \mathbf{k}(\tau), \quad (7)$$

where $\delta \mathbf{k}(\tau) = \delta \mathbf{k} e^{i\omega\tau}$ is the instantaneous displacement of valleys, which is determined by the time-dependent strain. $|\delta \mathbf{k}|$ represents the displacement amplitude. Note that $\cos(\omega\tau)$ in Eq. (3) has been extended into $e^{i\omega\tau}$ analytically. For the armchair ribbon under a uniaxial deformation, $\delta \mathbf{k}(\tau) = [\delta k_x^A(\tau), 0]$ (see Appendix B), with

$$\delta k_x^A(\tau) \approx -\xi\beta(1 + \sigma)\epsilon(\tau)/2a_0, \quad (8)$$

while for the zigzag one under the shear deformation, $\delta \mathbf{k}(\tau) = [\delta k_x^Z(\tau), 0]$ (see Appendix B), with

$$\delta k_x^Z(\tau) \approx -\xi\beta\gamma(\tau)/2a_0, \quad (9)$$

where $\xi = +1$ for valley K and $\xi = -1$ for valley K' . $\gamma(\tau) = \gamma_0 e^{i\omega\tau}$ denotes the strain parameter of the time-dependent shear strain and γ_0 is the amplitude of the strain. The displacements in Eqs. (8) and (9) and the corresponding pseudoelectric fields, referred to as $\mathbf{E}_x(\tau)$, are parallel to the x direction.

Theoretically, the ac charge current in Eq. (6) can be equivalently written as $J_y(\tau) = \sigma_{yx} E_x(\tau)$, where $E_x(\tau) = |\mathbf{E}_x(\tau)|$ is the strength of the pseudoelectric field. σ_{yx} denotes the Hall

pseudoconductance and can be calculated by

$$\sigma_{yx} = \frac{2e}{|\delta \mathbf{k}|} \sum_{\mathbf{k}, E_{kj} > E_{kj'}} \frac{\text{Im}[J_{jj'}^y(\mathbf{k})H'_{jj'}(\mathbf{k}, 0)](f_{kj} - f_{kj'})}{(E_{kj} - E_{kj'})^2 - \hbar^2\omega^2}. \quad (10)$$

On the other hand, the Hall pseudoconductance should also be equal to the valley Chern number $C_v = C_K - C_{K'}$ [20] in units of the conductance quantum e^2/h . Here, the valley-resolved Chern number $C_{K(K')}$ is defined to be the integral of Berry curvature over the neighborhood of the single valley K (K') [11,12],

$$C_{K(K')} = \frac{1}{2\pi} \int_{\text{Half BZ}} \Omega_{K(K')}(\mathbf{k}) d^2\mathbf{k}, \quad (11)$$

with the neighborhood as large as half of the Brillouin zone. One of the main aims of this paper is to figure out how well the Hall pseudoconductance from the linear response theory agrees with the valley Chern number.

III. RESULTS AND DISCUSSION

A. Hall pseudoconductance

In this section, we present the numerical results of Hall pseudoconductance. To open a gap, two types of mass terms in α - T_3 lattices are considered [21–23]:

$$M_1 = \begin{pmatrix} -m & 0 & 0 \\ 0 & 0 & 0 \\ 0 & 0 & m \end{pmatrix}, \quad M_2 = \begin{pmatrix} m & 0 & 0 \\ 0 & -m & 0 \\ 0 & 0 & m \end{pmatrix}. \quad (12)$$

The low-energy band structures are shown in Fig. 2. Note that, for $M = M_2$, the band structures are α independent. With a gap, the valley Chern number can be well defined when the intervalley scattering is ignorable. It has been shown that the valley Chern number of the α - T_3 lattice changes continuously with the parameter α , i.e., $C_v = 2 - \cos(2\varphi)$ for $M = M_1$ [11] and $C_v = \cos(2\varphi)$ for $M = M_2$ [12].

First, we focus on the zero-temperature and zero-frequency limit, $T = 0$ K and $\omega \rightarrow 0$. Equation (10) can be further simplified as

$$\sigma_{yx} = \frac{2e}{|\delta \mathbf{k}|} \sum_{\substack{\mathbf{k}, E_{kj} > \mu \\ E_{kj'} < \mu}} \frac{\text{Im}[J_{jj'}^y(\mathbf{k})H'_{jj'}(\mathbf{k}, 0)]}{(E_{kj} - E_{kj'})^2}. \quad (13)$$

The Fermi energy μ lies in the gap between the valence band and the middle flat band. Figure 3 shows the numerical results of the Hall pseudoconductance of armchair (zigzag) ribbons, under the time-dependent uniaxial (shear) strain. The Hall pseudoconductances are perfectly consistent with the valley Chern numbers in units of the conductance quantum e^2/h . For the mass term $M = M_1$, two quantized conductances appear at $\alpha = 0$ and $\alpha = 1$, with the values $\sigma_{yx} = e^2/h$ and $2e^2/h$, respectively. For $M = M_2$, the quantized Hall pseudoconductance appears at only $\alpha = 0$, with the value $\sigma_{yx} = e^2/h$. In both cases, when $0 < \alpha < 1$, the Hall pseudoconductances are continuous invariants which continuously vary with increasing α , but remain invariant against the fluctuation of other parameters.

Without loss of generality, we only show the numerical results of armchair ribbon in the following discussion.

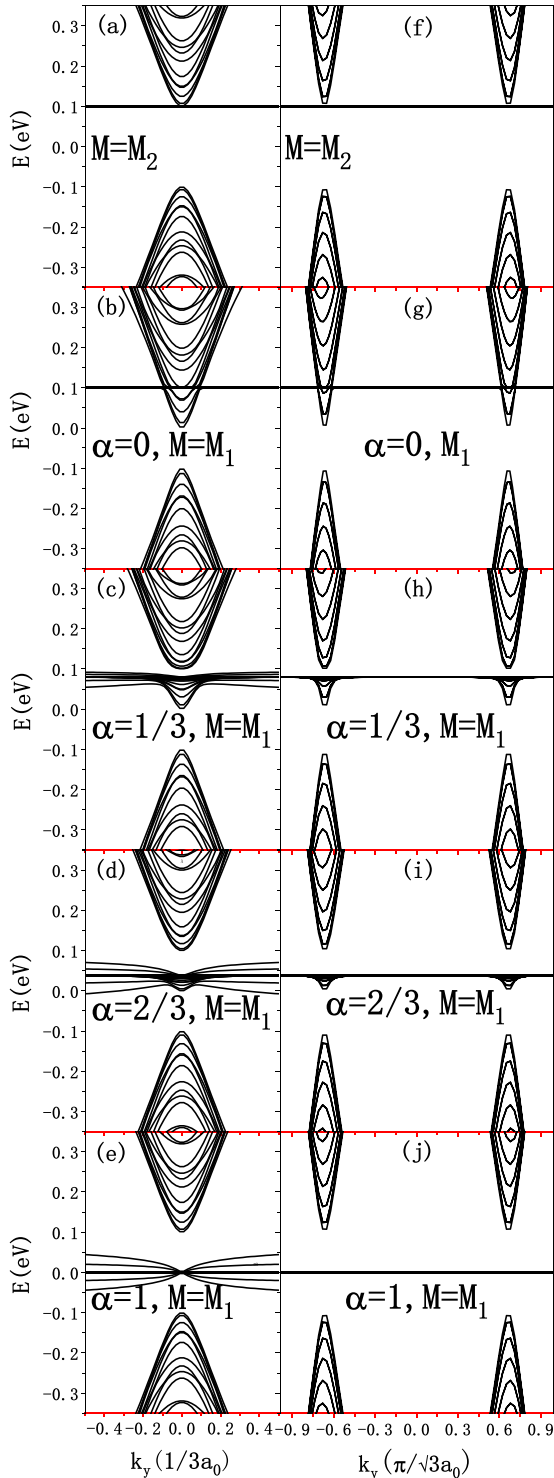


FIG. 2. The band structures of the (a)–(e) armchair and (f)–(j) zigzag α - T_3 ribbon ($N = 100$), with $k_x = 2\pi/(3\sqrt{3}a_0)$ and $k_x = 0$, respectively. The mass terms are set as $M = M_2$ for (a) and (f), and $M = M_1$ for the others. In all cases, $m = 0.1t_0$.

Figure 4(a) shows the temperature dependence of the Hall pseudoconductance. Obviously, the robustness against the thermal fluctuation is determined by the gap. For a mass $m = 0.005t_0$, the Hall pseudoconductance remains robust up to $T = 10$ K for $M = M_1$, while up to $T = 20$ K for $M = M_2$.

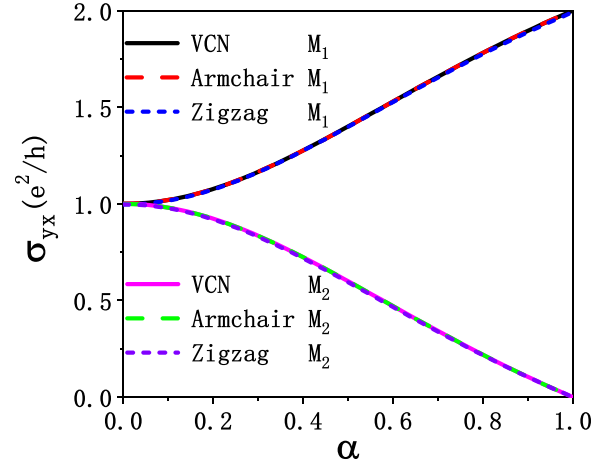


FIG. 3. The strain-related Hall pseudoconductance of the armchair and zigzag ribbons with different types of mass terms, as a consequence of the linear response theory. The parameters in the calculation are set as $N = 40$, $m = 0.001t_0$, $\omega = 0$. $\epsilon_0 = 1\%$ for the armchair ribbon and $\gamma_0 = 1\%$ for the zigzag ribbon. As a comparison, the analytic valley Chern numbers (VCNs) are also plotted.

This is because M_2 opens a larger gap with the same m . Figure 4(b) shows the conductance at low frequency ω at $T = 0$ K. It is shown that the zero-frequency limit remains well when $\hbar\omega \ll m$.

B. Robustness against disorders

To investigate the robustness of Hall pseudoconductance against long-range disorders, we add an on-site Gaussian disordered potential $U(\mathbf{r})$ to the supercells of ribbons [24–26],

$$U(\mathbf{r}) = \sum_{n=1}^{N_{\text{imp}}} U_n^{\text{imp}} \exp\left(-\frac{|\mathbf{r} - \mathbf{r}_n|^2}{2\lambda^2}\right), \quad (14)$$

where N_{imp} is the number of impurity centers. \mathbf{r}_n is the position of the impurity center, which is randomly selected from $3N$ sites of the supercells. The density of the impurity can be

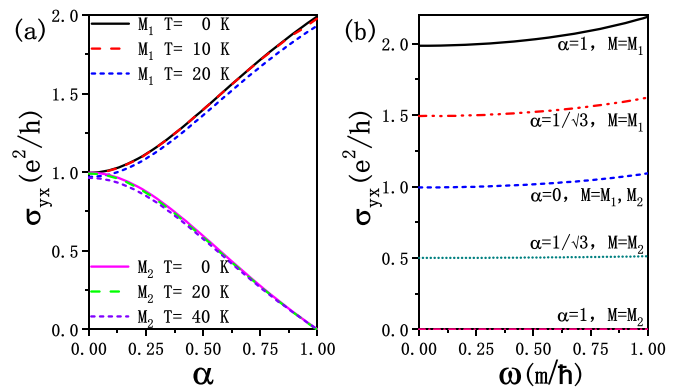


FIG. 4. (a) The Hall pseudoconductances of armchair ribbons with different types of masses and temperature. (b) The Hall conductance change with frequency ω of the time-dependent strain. The parameters are set as $N = 40$, $m = 0.005t_0$, $\omega = 0$, $\epsilon_0 = 1\%$.

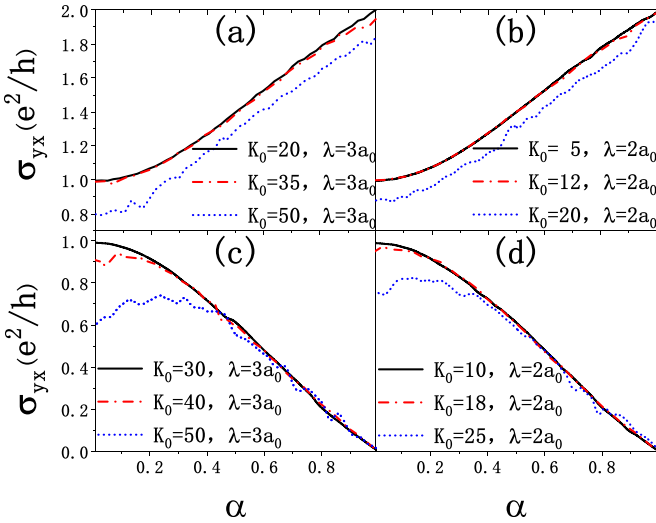


FIG. 5. The Hall pseudoconductances of armchair ribbons with different types of masses, K_0 and λ , in the limit of zero temperature and zero frequency. The mass term is $M = M_1$ for (a) and (b), and $M = M_2$ for (c) and (d). The parameters are set as $N = 40$, $m = 0.001t_0$, $\omega = 0$, $\epsilon_0 = 1\%$.

defined as $n_{\text{imp}} = N_{\text{imp}}/3N$. U_n^{imp} is the on-site energy of the impurity center at \mathbf{r}_n , with the value randomly chosen in the interval $[-\delta m/2, \delta m/2]$. λ denotes the screening coefficient. Similar to Refs. [26,27], the dimensionless strength of disorder for the quasi-one-dimensional supercell can be defined as $K_0 \approx \delta \sqrt{40.5 n_{\text{imp}} (\lambda/a_0)^2}$, where $\lambda \geq a_0$. We set $n_{\text{imp}} = 5\%$ in the calculation.

The numerical results are shown in Fig. 5. When the screening coefficients are fixed at $\lambda = 3a_0$ in Figs. 5(a) and 5(c), the Hall pseudoconductances remain robust against disorders with the strength up to $K_0 = 20$ for $M = M_1$, and up to $K_0 = 30$ for $M = M_2$. When the screening coefficients are fixed at $\lambda = 2a_0$ in Figs. 5(b) and 5(d), the Hall pseudoconductances remain robust against disorders with the strength only up to $K_0 = 5$ for $M = M_1$, and up to $K_0 = 10$ for $M = M_2$. It verifies that the Hall pseudoconductance is robust against long-range disorders with large λ , while it is sensitive to short-range disorders with small λ .

IV. CONCLUSION

In this paper, we propose that an ac charge current can be generated by applying time-dependent strains to α - T_3 ribbons. The corresponding Hall pseudoconductance equals the continuously tunable valley Chern number at the low-frequency limit and is robust against long-range disorders. This finding advances the understanding of the relation between invariants and topology, and also provides a scheme to test the quantum valley Hall effect.

ACKNOWLEDGMENTS

The work described in this paper is supported by the National Natural Science Foundation of China (NSFC, Grants No. 12174077 and No. 12174051), the National Natural Science Foundation of Guangdong Province (Grant

No. 2021A1515012363), and the Bureau of Education of Guangzhou Municipality (Grant No. 202255464).

APPENDIX A: THE TIGHT-BINDING HAMILTONIAN OF THE ZIGZAG RIBBON

For the zigzag ribbon, the tight-binding (TB) Hamiltonian reads

$$H_Z(\mathbf{k}) = \begin{bmatrix} I_1^Z & O_1^Z & 0 & \cdots & \cdots & \cdots & O_{1N}^Z \\ O_1^{Z\dagger} & I_2^Z & O_2^Z & \cdots & \cdots & \cdots & 0 \\ 0 & O_2^{Z\dagger} & I_3^Z & \cdots & \cdots & \cdots & 0 \\ \cdots & \cdots & \cdots & \cdots & \cdots & \cdots & \cdots \\ \cdots & \cdots & \cdots & O_{n-1}^{Z\dagger} & I_n^Z & O_n^Z & \cdots \\ \cdots & \cdots & \cdots & \cdots & \cdots & \cdots & \cdots \\ O_{1N}^{Z\dagger} & 0 & 0 & \cdots & \cdots & O_{N-1}^{Z\dagger} & I_N^Z \end{bmatrix}, \quad (\text{A1})$$

where

$$I_n^Z = M + \begin{pmatrix} 0 & t_{ab}^z & 0 \\ t_{ab}^{z*} & 0 & t_{bc}^z \\ 0 & t_{ab}^{z*} & 0 \end{pmatrix},$$

$$O_n^Z = \begin{pmatrix} 0 & t_{ab} & 0 \\ 0 & 0 & t_{bc} \\ 0 & 0 & 0 \end{pmatrix}, \quad O_{1N}^Z = \begin{pmatrix} 0 & t_{ab}^o & 0 \\ 0 & 0 & t_{bc}^o \\ 0 & 0 & 0 \end{pmatrix},$$

where $t_{ab(bc)}^z = 2t_{ab(bc)} \cos(k_y \frac{\sqrt{3}a_0}{2})$ is the hopping parameter of the zigzag ribbon. For a wide ribbon, $t_{ab(bc)}^o = t_{ab(bc)} \cos(k_y \frac{\sqrt{3}a_0}{2}) e^{iN \frac{3a_0}{2} k_x}$. The band structure of the zigzag ribbon is shown in Fig. 1(b) in the main text, without considering the mass term.

When a time-dependent shear strain is applied to the zigzag ribbon along the zigzag direction, the deformed supercell is shown in Fig. 1(f) in the main text, and the instantaneous deformed bond lengths [Fig. 1(f)] are respectively given as [15]

$$d_1 = a_0 \sqrt{1 + \delta_1}, \quad d_2 = a_0 \sqrt{1 + \delta_2},$$

$$d_3 = a_0 \sqrt{1 + \delta_3}, \quad (\text{A2})$$

where $\delta_1 = -\gamma(\tau)\sqrt{3}/2$, $\delta_2 = \gamma(\tau)^2$, $\delta_3 = \gamma(\tau)\sqrt{3}/2$. $\gamma(\tau) = \gamma_0 \cos(\omega\tau)$ is the strain parameter of the time-dependent shear strain. γ_0 and ω are the amplitude and frequency of the strain. The perturbation Hamiltonian can be obtained as

$$H'_Z(\mathbf{k}, \tau) = \begin{bmatrix} I_1^{Z'} & 0 & 0 & \cdots & \cdots & \cdots & 0 \\ 0 & I_2^{Z'} & 0 & \cdots & \cdots & \cdots & 0 \\ 0 & 0 & I_3^{Z'} & \cdots & \cdots & \cdots & 0 \\ \cdots & \cdots & \cdots & \cdots & \cdots & \cdots & \cdots \\ \cdots & \cdots & \cdots & 0 & I_n^{Z'} & 0 & \cdots \\ \cdots & \cdots & \cdots & \cdots & \cdots & \cdots & \cdots \\ 0 & 0 & 0 & \cdots & \cdots & 0 & I_N^{Z'} \end{bmatrix}, \quad (\text{A3})$$

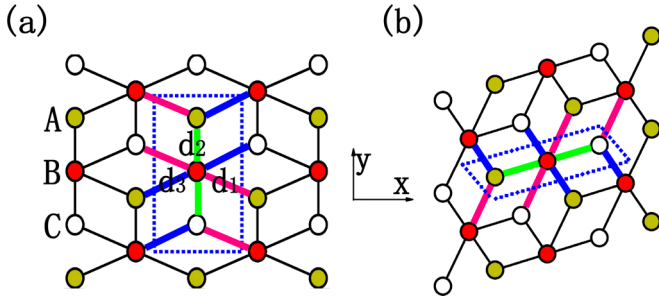


FIG. 6. Schematic of the α - T_3 lattices after (a) uniaxial and (b) shear deformations, with both strains applied along the zigzag direction. The bond lengths are changed from a_0 to d_χ , $\chi = 1$ (pink bonds), 2 (green bonds), 3 (blue bonds).

where

$$I_{2n-1}^Z = I_{2n}^{Z*} = \begin{pmatrix} 0 & t_{ab}^{z'} & 0 \\ t_{ab}^{z'*} & 0 & t_{bc}^{z'} \\ 0 & t_{bc}^{z'*} & 0 \end{pmatrix}.$$

Note that the hopping terms between different cells can be canceled under a first-order approximation, and $t_{ab(bc)}^{z'} = -i\frac{\sqrt{3}}{2}\beta\gamma(\tau)t_{ab(bc)}\sin(k_y\frac{\sqrt{3}a_0}{2})$ as the intracell hopping parameter.

APPENDIX B: DISPLACEMENTS OF VALLEYS

The uniaxial and shear deformed lattices are shown in Figs. 6(a) and 6(b), respectively. At this part, the strains are time independent, and fixed at $\tau = 0$. The unit cell of the α - T_3 lattice is shown in the blue dotted rectangle in Fig. 6. Without loss of generality, we focus on the displacement of valley K in this Appendix.

1. *The uniaxial strain is applied along the zigzag direction.*

The electronic states for the uniaxial deformed α - T_3 lattice can be represented by three-component wave functions $\Psi = (\psi_A, \psi_B, \psi_C)^T$, and the Hamiltonian can be written as

$$H_U(\mathbf{k}) = \begin{pmatrix} 0 & U_{ab} & 0 \\ U_{ab}^* & 0 & U_{bc} \\ 0 & U_{bc}^* & 0 \end{pmatrix}, \quad (\text{B1})$$

where

$$U_{ab(bc)} = t_{ab(bc)}^{(U1)} e^{-i(\sqrt{3}k_x a_0/2 - k_y a_0/2)} + t_{ab(bc)}^{(U2)} e^{-ik_y a_0} + t_{ab(bc)}^{(U3)} e^{i(\sqrt{3}k_x a_0/2 + k_y a_0/2)}$$

denotes the hopping parameter between sites A (B) and B (C), where $t_{ab(bc)}^{(U\chi)} = t_{ab(bc)} \exp[-\beta(d_\chi/a_0 - 1)]$, with $\chi = 1, 2, 3$. d_χ is shown in Fig. 6(a) and the values can be found in Eq. (3) in the main text. Under the first-order approximation, the conduction and valence band can be respectively given as

$$E_\pm^U = \pm t_0 [e^{2\beta\sigma\epsilon} + 2e^{-\beta(3-\sigma)\epsilon/2} [1 + \cos(\sqrt{3}k_x a_0)] + 4e^{-\beta(3-5\sigma)\epsilon/4} \cos(\sqrt{3}k_x a_0/2) \cos(3k_y a_0/2)]^{1/2}. \quad (\text{B2})$$

We define $(k_x, k_y) = (\frac{4\pi}{3\sqrt{3}a_0}, 0)$ as one of the positions of valley K of the pristine lattice. After uniaxial deformation, the

position of valley K would change to $(k_x^U, 0)$, with

$$k_x^U = \frac{2}{\sqrt{3}a_0} \arccos\left(-\frac{1}{2}e^{-3\beta(1+\sigma)\epsilon/4}\right), \quad (\text{B3})$$

obtained from Eq. (B2). So, the displacement would be $[\delta k_x^A(K), 0]$, with

$$\begin{aligned} \delta k_x^A(K) &= k_x^U - \frac{4\pi}{3\sqrt{3}a_0} \\ &= \frac{2}{\sqrt{3}a_0} \left[\arccos\left(-\frac{1}{2}e^{-3\beta(1+\sigma)\epsilon/4}\right) - \frac{2\pi}{3} \right] \\ &\approx -\beta(1+\sigma)\epsilon/2a_0. \end{aligned} \quad (\text{B4})$$

2. *The shear strain is applied along the zigzag direction.*

The Hamiltonian can be written as

$$H_S(\mathbf{k}) = \begin{pmatrix} 0 & S_{ab} & 0 \\ S_{ab}^* & 0 & S_{bc} \\ 0 & S_{bc}^* & 0 \end{pmatrix}, \quad (\text{B5})$$

where

$$\begin{aligned} S_{ab(bc)} &= t_{ab(bc)}^{(S1)} e^{-i(k_x a_0/2 - \sqrt{3}k_y a_0/2)} + t_{ab(bc)}^{(S2)} e^{ik_x a_0} \\ &\quad + t_{ab(bc)}^{(S3)} e^{-i(k_x a_0/2 + \sqrt{3}k_y a_0/2)} \end{aligned}$$

denotes the hopping parameter between sites A (B) and B (C), with $t_{ab(bc)}^{(S\chi)} = t_{ab(bc)} \exp[-\beta(d_\chi/a_0 - 1)]$, with $\chi = 1, 2, 3$. d_χ can be found in Eq. (A2) and shown in Fig. 6(b). Under the first-order approximation, the conduction and valence band can be respectively obtained as

$$\begin{aligned} E_\pm^S &= \pm t_0 [1 + 2 \cosh(2D) + 2 \cos(\sqrt{3}k_y a_0) \\ &\quad + \cos(3k_x a_0/2 - \sqrt{3}k_y a_0/2) e^D \\ &\quad + \cos(3k_x a_0/2 + \sqrt{3}k_y a_0/2) e^{-D}]^{1/2}, \end{aligned} \quad (\text{B6})$$

where $D = \sqrt{3}\beta\gamma/4$. After shear deformation, the valley K at $(0, \frac{4\pi}{3\sqrt{3}a_0})$ will shift to $(k_x^S, \frac{4\pi}{3\sqrt{3}a_0})$, with

$$k_x^S \approx -\beta\gamma/2a_0, \quad (\text{B7})$$

obtained from Eq. (B6). The displacement would be $[\delta k_x^Z(K), 0]$, with

$$\delta k_x^Z(K) = k_x^S - 0 \approx -\beta\gamma/2a_0. \quad (\text{B8})$$

Similarly, the corresponding displacements of valley K' can be respectively given as $[\delta k_x^A(K'), 0]$ and $[\delta k_x^Z(K'), 0]$, with

$$\delta k_x^A(K') = -\left(k_x^U - \frac{4\pi}{3\sqrt{3}a_0}\right) \approx \beta(1+\sigma)\epsilon/2a_0 \quad (\text{B9})$$

and

$$\delta k_x^Z(K') = -(k_x^S - 0) \approx \beta\gamma/2a_0. \quad (\text{B10})$$

APPENDIX C: DEDUCTION OF EQ. (6)

When the time-dependent strain is applied to the α - T_3 ribbons, the perturbation Hamiltonian can be further written as $H'(\mathbf{k}, \tau) = B(\mathbf{k}, \tau)F(\tau)$, where $F(\tau) = e^{i\omega\tau}$ is assumed to be a scalar field coupled to an observable $B(\mathbf{k}, \tau) = B(\mathbf{k})$. We introduce the field operator $\Psi = \sum_{\mathbf{k}j} \phi_{\mathbf{k}j} e^{i\mathbf{k}\mathbf{r}} \phi_{\mathbf{k}j}$, with $\phi_{\mathbf{k}j}$

being the annihilation operator. The current operator and the perturbation Hamiltonian can be written as

$$J_y = \sum_{kjj'} J_{jj'}^y \phi_{kj}^\dagger \phi_{kj}, \quad H'(\mathbf{k}, \tau) = \sum_{kjj'} H'_{jj'}(\mathbf{k}, \tau) \phi_{kj}^\dagger \phi_{kj}, \quad (\text{C1})$$

where $J_{jj'}^y(\mathbf{k}) = \frac{e}{\hbar} \phi_{kj}^\dagger \frac{\partial H(\mathbf{k})}{\partial k_y} \phi_{kj}$ and $H'_{jj'}(\mathbf{k}, \tau) = \phi_{kj}^\dagger H'(\mathbf{k}, \tau) \phi_{kj}$, respectively. According to linear response theory, the ac charge current response along the longitudinal direction (y direction) can be obtained as

$$J_y(\tau) = \int_{-\infty}^{+\infty} G_{JB}^R(\tau - \tau') F(\tau') d\tau', \quad (\text{C2})$$

where

$$G_{JB}^R(\tau - \tau') = -i\theta(\tau - \tau') \langle [J_y(\tau), B(\mathbf{k}, \tau')] \rangle \quad (\text{C3})$$

is a retarded Green's function. After Fourier transform,

$$\begin{aligned} J_y(\omega') &= \iint_{-\infty}^{+\infty} G_{JB}^R(\tau - \tau') F(\tau') e^{-i\omega'\tau} d\tau' d\tau \\ &= \iint_{-\infty}^{+\infty} G_{JB}^R(\tau - \tau') e^{-i\omega'(\tau - \tau')} F(\tau') e^{-i\omega'\tau'} d\tau' d\tau \\ &= 2\pi G_{JB}^R(\omega') \delta(\omega' - \omega). \end{aligned} \quad (\text{C4})$$

$G_{JB}^R(\omega')$ can be obtained from the finite-temperature Green's function $M_{JB}(\tau) = \langle \mathcal{T} J_y(\tau) B(\mathbf{k}, 0) \rangle$, where \mathcal{T} is the time-ordering operator. For $\tau > 0$ without loss of generality, we can obtain

$$\begin{aligned} M_{JB}(\tau) &= \left\langle \mathcal{T} \sum_{kjj'} J_{jj'}^y \phi_{kj}^\dagger(\tau) \phi_{k'j'}(\tau) \right. \\ &\quad \left. \times \sum_{kk'i'i'j'j'} B_{i'i'}(\mathbf{k}') \phi_{k'i}^\dagger(0) \phi_{k'i'}(0) \right\rangle \\ &= \sum_{kk'i'i'j'j'} J_{jj'}^y B_{i'i'}(\mathbf{k}') \delta_{kk'} \delta_{j'i'} \delta_{j'i} \\ &\quad \times \langle \mathcal{T} \phi_{kj}^\dagger(\tau) \phi_{k'j'}(\tau) \phi_{k'i}^\dagger(0) \phi_{k'i'}(0) \rangle \\ &= - \sum_{kjj'} J_{jj'}^y B_{j'j}(\mathbf{k}) \langle \phi_{kj}(0) \phi_{kj}^\dagger(\tau) \rangle \langle \phi_{k'j'}(\tau) \phi_{k'j'}^\dagger(0) \rangle \\ &= - \sum_{kjj'} J_{jj'}^y B_{j'j}(\mathbf{k}) \varrho_{kj}(-\tau) \varrho_{k'j'}(\tau), \end{aligned} \quad (\text{C5})$$

where $\varrho_{kj}(\tau)$ is the Green's function of the free Bloch electrons. We can expand $M_{JB}(\tau)$ in the range $0 \leq \tau \leq \chi$ as a

Fourier series and the Fourier coefficients would be

$$\begin{aligned} M_{JB}(\omega_n) &= \int_0^\chi e^{-\omega_n \tau} M_{JB}(\tau) d\tau \\ &= - \int_0^\chi e^{-\omega_n \tau} \sum_{kjj'} J_{jj'}^y B_{j'j}(\mathbf{k}) \varrho_{kj}(-\tau) \varrho_{k'j'}(\tau) d\tau \\ &= - \sum_{kjj'\omega_1\omega_2} \int_0^\chi e^{-\omega_n \tau} J_{jj'}^y B_{j'j}(\mathbf{k}) \frac{1}{\chi} \varrho_{kj}(\omega_1) e^{-\omega_1 \tau} \\ &\quad \times \frac{1}{\chi} \varrho_{k'j'}(\omega_2) e^{\omega_2 \tau} \\ &= - \frac{1}{\chi} \sum_{kjj'\omega_1} J_{jj'}^y B_{j'j}(\mathbf{k}) \varrho_{kj}(\omega_1) \varrho_{k'j'}(\omega_1 + \omega_n) \\ &= - \sum_{kjj'\omega_1} \frac{J_{jj'}^y B_{j'j}(\mathbf{k})}{\chi} \frac{1}{\omega_1 - E_{k'j'} + \mu} \\ &\quad \times \frac{1}{\omega_1 + \omega_n - E_{k'j'} + \mu} \\ &= - \sum_{kjj'} \frac{J_{jj'}^y B_{j'j}(\mathbf{k}) (f_{kj} - f_{k'j'})}{\omega_n + E_{kj} - E_{k'j'}}. \end{aligned} \quad (\text{C6})$$

Here, we neglect the reduced Planck constant by setting $\hbar = 1$. As $G_{JB}^R(\omega') = M_{JB}(\omega' + i\eta)$, where η is a positive infinitesimal,

$$G_{JB}^R(\omega') = \sum_{kjj'} \frac{J_{jj'}^y B_{j'j}(\mathbf{k}) (f_{kj} - f_{k'j'})}{\omega' + E_{kj} - E_{k'j'} + i\eta}. \quad (\text{C7})$$

In the end, the ac charge current can be obtained as

$$\begin{aligned} J_y(\tau) &= \frac{1}{2\pi} \int_{-\infty}^{+\infty} J_y(\omega') e^{i\omega'\tau} d\omega' \\ &= \int_{-\infty}^{+\infty} G_{JB}^R(\omega') \delta(\omega' - \omega) e^{i\omega'\tau} d\omega' \\ &= G_{JB}^R(\omega) e^{i\omega\tau} \\ &= - \sum_{kjj'} \frac{J_{jj'}^y B_{j'j}(\mathbf{k}) e^{i\omega\tau} (f_{kj} - f_{k'j'})}{\omega + E_{kj} - E_{k'j'} + i\eta} \\ &= - \sum_{kjj'} \frac{J_{jj'}^y(\mathbf{k}) H'_{j'j}(\mathbf{k}, \tau) (f_{kj} - f_{k'j'})}{\omega + E_{kj} - E_{k'j'} + i\eta}. \end{aligned} \quad (\text{C8})$$

This is Eq. (6) in the main text.

- [1] K. von Klitzing, *Rev. Mod. Phys.* **58**, 519 (1986).
- [2] K. von Klitzing, *Philos. Trans. R. Soc. A* **363**, 2203 (2005).
- [3] R. Laughlin, *Science* **242**, 525 (1988).
- [4] H. L. Stormer, D. C. Tsui, and A. C. Gossard, *Rev. Mod. Phys.* **71**, S298 (1999).
- [5] D. Xiao, W. Yao, and Q. Niu, *Phys. Rev. Lett.* **99**, 236809 (2007).

- [6] D. Xiao, M.-C. Chang, and Q. Niu, *Rev. Mod. Phys.* **82**, 1959 (2010).
- [7] E. Illes, Properties of the α - T_3 Model, Ph.D. thesis, University of Guelph, 2017.
- [8] E. Illes and E. J. Nicol, *Phys. Rev. B* **95**, 235432 (2017).
- [9] T. Biswas and T. K. Ghosh, *J. Phys.: Condens. Matter* **28**, 495302 (2016).

- [10] J. Wang, J. F. Liu, and C. S. Ting, *Phys. Rev. B* **101**, 205420 (2020).
- [11] E. V. Gorbar, V. P. Gusynin, and D. O. Oriekhov, *Phys. Rev. B* **99**, 155124 (2019).
- [12] F. Piéchon, J.-N. Fuchs, A. Raoux, and G. Montambaux, *J. Phys.: Conf. Ser.* **603**, 012001 (2015).
- [13] M. Sui, G. Chen, L. Ma, W.-Y. Shan, D. Tian, K. Watanabe, T. Taniguchi, X. Jin, W. Yao, D. Xiao *et al.*, *Nat. Phys.* **11**, 1027 (2015).
- [14] A. Vaezi, N. Abedpour, R. Asgari, A. Cortijo, and M. A. H. Vozmediano, *Phys. Rev. B* **88**, 125406 (2013).
- [15] V. M. Pereira, A. H. C. Neto, and N. M. R. Peres, *Phys. Rev. B* **80**, 045401 (2009).
- [16] T. Fujita, M. Jalil, and S. Tan, *Appl. Phys. Lett.* **97**, 043508 (2010).
- [17] A. Filusch, A. R. Bishop, A. Saxena, G. Wellein, and H. Fehske, *Phys. Rev. B* **103**, 165114 (2021).
- [18] N. E. Firsova and Y. A. Firsov, *J. Phys. D* **45**, 435102 (2012).
- [19] A. Bhat, S. Alsaleh, D. Momeni, A. Rehman, Z. Zaz, M. Faizal, A. Jellal, and L. Alasfar, *Eur. Phys. J. B* **91**, 174 (2018).
- [20] S. Bhowal and G. Vignale, *Phys. Rev. B* **103**, 195309 (2021).
- [21] R. Shen, L. B. Shao, B. Wang, and D. Y. Xing, *Phys. Rev. B* **81**, 041410(R) (2010).
- [22] C. Xu, G. Wang, Z. H. Hang, J. Luo, C. T. Chan, and Y. Lai, *Sci. Rep.* **5**, 18181 (2015).
- [23] C. Shang, Y. Zheng, and B. A. Malomed, *Phys. Rev. A* **97**, 043602 (2018).
- [24] N. H. Shon and T. Ando, *J. Phys. Soc. Jpn.* **67**, 2421 (1998).
- [25] C. H. Lewenkopf, E. R. Mucciolo, and A. H. Castro Neto, *Phys. Rev. B* **77**, 081410(R) (2008).
- [26] A. Rycerz, J. Tworzydło, and C. Beenakker, *Europhys. Lett.* **79**, 57003 (2007).
- [27] E. R. Mucciolo, A. H. C. Neto, and C. H. Lewenkopf, *Phys. Rev. B* **79**, 075407 (2009).